

## Study of $B$ and $B_s$ Decays at Belle

---

**N. K. Nisar**<sup>1,\*</sup>

*Brookhaven National Laboratory,  
Upton, New York, 11973*

*E-mail:* [nnellikun@bnl.gov](mailto:nnellikun@bnl.gov)

We report results on the search for  $B_s \rightarrow \eta'\eta$  decay, and the searches for  $B^0 \rightarrow$  invisible and  $B^0 \rightarrow$  invisible  $\gamma$  decays. The former result is based on a data sample of  $121.4 \text{ fb}^{-1}$  recorded at the  $Y5S$  resonance while the later results are obtained from a  $711 \text{ fb}^{-1}$  of data sample collected at  $Y4S$  resonance with the Belle detector at the KEKB  $ee^-$  collider. We observe no significant signal for the decays and set upper limit on their branching fractions at 90% confidence level of  $\mathcal{B}B_s \rightarrow \eta'\eta < 7.1 \times 10^{-5}$ ,  $\mathcal{B}B^0 \rightarrow$  invisible  $< 7.8 \times 10^{-5}$  and  $\mathcal{B}B^0 \rightarrow$  invisible  $\gamma < 1.6 \times 10^{-5}$ .

*40th International Conference on High Energy physics - ICHEP2020  
July 28 - August 6, 2020  
Prague, Czech Republic (virtual meeting)*

---

<sup>1</sup>On behalf of the Belle Collaboration  
\*Speaker

## 1. Introduction

In the Standard Model (SM),  $B_s^0 \rightarrow \eta' \eta$  decay proceeds via tree-level  $b \rightarrow u$  and penguin  $b \rightarrow s$  transitions. Penguin transitions are sensitive to Beyond-the-Standard-Model (BSM) physics scenarios and could affect its branching fraction and  $CP$  asymmetry [1]. Once the branching fractions for two-body decays  $B_{s,d} \rightarrow \eta \eta, \eta \eta', \eta' \eta'$  are measured, and the theoretical uncertainties are reduced, it would be possible to extract  $CP$  violating parameters from the data using the formalism based on  $SU(3)/U(3)$  symmetry [2]. The formalism requires at least four of these six branching fractions and the result on  $B_s^0 \rightarrow \eta' \eta$  is a potential input. The predicted branching fractions of the decays  $B^0 \rightarrow \text{invisible}$  and  $B^0 \rightarrow \text{invisible } \gamma$ , where “invisible” defined as particles that leave no signal in the Belle detector, could be as high as  $10^{-6} - 10^{-7}$  in the New Physics (NP) models [3, 4]. Decays with similar signature such as  $B^0 \rightarrow \gamma \nu \bar{\nu}$  and  $B^0 \rightarrow \nu \bar{\nu} \nu \bar{\nu}$  are highly suppressed in the SM [5–7]. A very low background from the SM indicates that a signal of  $B^0 \rightarrow \text{invisible } \gamma$  in the current B-factory data would indicate NP.

## 2. Belle detector

The Belle detector [8] was a large-solid-angle magnetic spectrometer that operated at the KEKB asymmetric-energy  $ee^-$  collider [9]. The detector components include a tracking system comprising a silicon vertex detector (SVD) and a central drift chamber (CDC), a particle identification (PID) system that consists of a barrel-like arrangement of time-of-flight scintillation counters (TOF) and an array of aerogel threshold Cherenkov counters (ACC), and a CsI(Tl) crystal-based electromagnetic calorimeter (ECL). All these components are located inside a superconducting solenoid coil that provides a 1.5 T magnetic field. Outside the coil, the  $K_L^0$  and muon detector (KLM) is instrumented to detect  $K_L^0$  mesons and to identify muons.

## 3. Search for the Decay $B_s^0 \rightarrow \eta' \eta$

In this paper we report the preliminary result of the first search for the decay  $B_s^0 \rightarrow \eta' \eta$  using the full Belle data sample of  $121.4 \text{ fb}^{-1}$  collected at the  $\Upsilon 5S$  resonance. The  $\Upsilon 5S$  decays into  $B_s^{*0} \bar{B}_s^{*0}, B_s^{*0} \bar{B}_s^0$  or  $B_s^0 \bar{B}_s^{*0}$ , and  $B_s^0 \bar{B}_s^0$  pairs followed by the decays of the excited vector states to  $B_s^0$ , by emitting a photon. Our data sample contains  $6.53 \pm 0.66 \times 10^6$   $B_s^{*0} \bar{B}_s^{*0}$  pairs [10]. A set of Monte Carlo (MC) simulated events are used for the selection optimization and estimation of reconstruction efficiency.

We reconstruct  $\eta$  candidates using pairs of photons of energy that exceeds 50 (100) MeV in the barrel (end-cap) region of the ECL and requiring the invariant mass to be in the range  $515 \leq M_{\gamma\gamma} \leq 580 \text{ MeV}c^2$ . Candidates for the decay  $\eta' \rightarrow \pi \pi^- \eta$  are reconstructed using pairs of oppositely-charged pions and  $\eta$ . We require the reconstructed  $\eta'$  invariant mass to be in the range  $920 \leq M_{\pi\pi^- \eta} \leq 980 \text{ MeV}c^2$ . To identify  $B_s^0 \rightarrow \eta' \eta$  candidates we use beam-energy constrained  $B_s^0$  mass,  $M_{bc} = \sqrt{E_{\text{beam}}^2 - p_{B_s}^2}$ , the energy difference,  $\Delta E = E_{B_s} - E_{\text{beam}}$ , and the reconstructed invariant mass of the  $\eta'$ , where  $E_{\text{beam}}, p_{B_s}$  and  $E_{B_s}$  are the beam energy, the momentum magnitude and the reconstructed energy of  $B_s^0$  candidate, respectively.

The primary source of background are  $ee^- \rightarrow q\bar{q}$  ( $q = u, d, c, s$ ) continuum events. Because of large initial momenta of the light quarks, continuum events exhibit a “jet-like” event shape, while

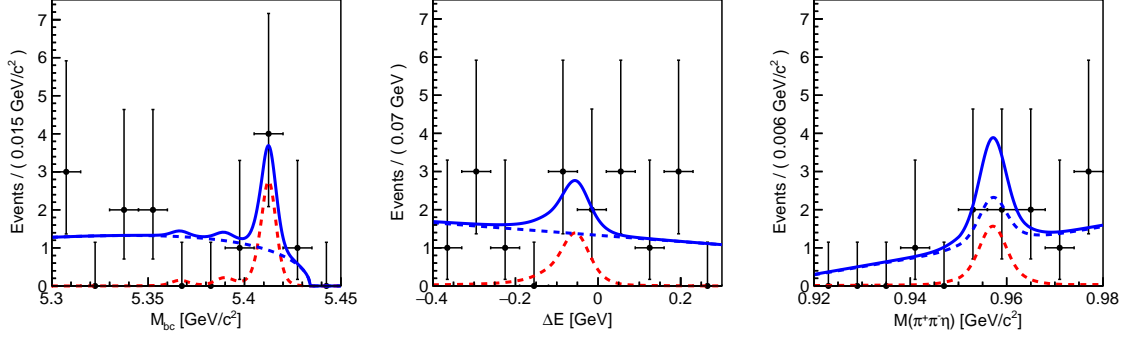


**Figure 1:** Signal-region projections of 3D fit to  $B_s^0 \rightarrow \eta' \eta$  data. Points with error bars represent data, blue solid curves show the resulting fit-projection, while the red dash-dotted and blue dash-dotted curves show the signal and background components.

$B_s^{*0} \bar{B}_s^{*0}$  events are distributed isotropically. We use modified Fox-Wolfram moments [11], which describe the topology of the event, to discriminate between signal and continuum background.

To extract the signal yield, we perform an unbinned extended maximum likelihood fit to the three-dimensional (3D) distribution of  $M_{bc}$ ,  $\Delta E$ , and  $M_{\pi\pi\eta}$ . MC sample is used to determine signal and background probability density functions (PDF). We use  $B^0 \rightarrow \eta' K_S^0$  data recorded at the  $Y4S$  resonance to adjust the PDF shape parameters used to describe the signal.

To test and validate our fitting model, ensemble tests are performed by generating MC pseudo-experiments using PDFs obtained from the simulation and the  $B^0 \rightarrow \eta' K_S^0$  data. We use the results of pseudoexperiments to construct classical confidence intervals using Neyman construction [12]. These confidence intervals are then used to prepare a classical confidence belt [13] and used to make a statistical interpretation of the results obtained from fit to data.

We obtain  $2.7 \pm 2.5$  signal and  $57.3 \pm 7.8$  background events from the 3D fit to data. We show the signal-region projections of the fit in Fig. 1. We observe no signal and estimate the 90% confidence-level (CL) upper limit on the branching fraction of the decay  $B_s^0 \rightarrow \eta' \eta$  using the frequentist approach [12] and the following formula:

$$\mathcal{B} B_s^0 \rightarrow \eta' \eta < \frac{N_{\text{UL}}^{90\%}}{2 \cdot N_{B_s^{*0} \bar{B}_s^{*0}} \cdot \varepsilon \cdot \mathcal{B}_{\text{dp}}}, \quad (1)$$

where  $N_{B_s^{*0} \bar{B}_s^{*0}}$  is the number of  $B_s^{*0} \bar{B}_s^{*0}$  pairs in the full Belle data sample,  $\varepsilon$  is the overall reconstruction efficiency for the signal  $B_s^0$  decay, and  $\mathcal{B}_{\text{dp}}$  is the product of the secondary branching fractions for all daughter particles in our final state. Further,  $N_{\text{UL}}^{90\%}$  is the expected signal yield at 90% CL obtained from the confidence belt, which is approximately 6 events. Using Eq. (1) we obtain a 90% CL upper limit on the branching fraction of  $\mathcal{B} B_s^0 \rightarrow \eta' \eta < 7.1 \times 10^{-5}$ . The total systematic uncertainty on the upper limit is estimated to be 17%.

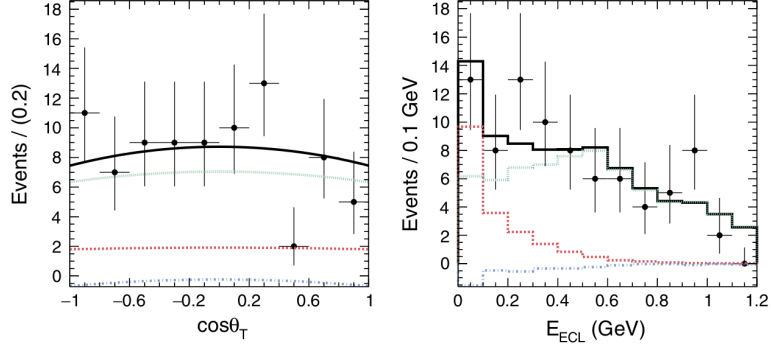


**Figure 2:** Projections of the fit result on  $\cos\theta_T$  (left) and  $E_{\text{ECL}}$  (right) for  $B^0 \rightarrow \text{invisible}$ . Points with error bars are data, black solid line is the fit result, red dotted line is the signal component, green short-dashed line is the generic  $B$  background component and blue dash-dotted line is the non- $B$  background component.

#### 4. Search for $B^0$ decays to invisible final states $\gamma$

These searches are based on a data sample containing  $772 \times 10^6 B\bar{B}$  pairs accumulated at the  $\Upsilon 4S$  resonance, corresponding to an integrated luminosity of  $711 \text{ fb}^{-1}$ . Ten million MC simulated events for  $B^0 \rightarrow \nu\bar{\nu}$  and  $B^0 \rightarrow \nu\bar{\nu}\gamma$  decays are generated and used to determine signal efficiency and optimize signal event selection.

Since the signal side particle, except photon, cannot be detected, the other  $B$  meson in the event ( $B_{\text{tag}}$ ) is reconstructed. Then the signal is searched in the remaining part of the event.  $B_{\text{tag}}$  mesons are reconstructed from 494 hadronic decay modes by assigning signal probability to reconstructed particles using a neural network (NN) package [14]. After reconstruction of  $B_{\text{tag}}$ , no extra particles but photons are expected in the event. Thus events with extra tracks,  $\pi^0$ s, or  $K_L^0$ s are rejected.

The sum of all remaining energies of ECL clusters that are not associated with  $B_{\text{tag}}$  daughters and signal photons in case of  $B^0 \rightarrow \text{invisible } \gamma$ , denoted by  $E_{\text{ECL}}$ , is a strong variable to identify signal events. Since the distribution for signal events peaks at zero, the  $E_{\text{ECL}}$  signal box is defined as  $E_{\text{ECL}} < 0.3 \text{ GeV}$  and the sideband is defined as  $0.3 \text{ GeV} < E_{\text{ECL}} < 1.2 \text{ GeV}$ . Continuum events are the dominant source of background (Non- $B$ ) followed by  $B\bar{B}$  decay with a  $b \rightarrow c$  transition (Generic  $B$ ). Two NNs are implemented to suppress these backgrounds.

A two dimensional (2D) extended unbinned maximum likelihood fit is applied with fitting variables  $E_{\text{ECL}}$  and  $\cos\theta_T$  to extract signal yield for the decay  $B^0 \rightarrow \text{invisible}$ . Here  $\cos\theta_T$  is the cosine of the angle between the two thrust axes in the  $ee^-$  c.m. frame. The two thrust axes are defined as the directions that maximizes the longitudinal momenta of  $B_{\text{tag}}$  daughters and particles in the remaining part of the event. All PDFs are obtained from signal MC and off-resonance data. The projections of the 2D fit results are shown in Fig. 2 and the corresponding fitting yields for each component are listed in Table. 1. No significant signal is observed and a 90% CL upper limit on the branching fraction is estimated to be  $\mathcal{B} B^0 \rightarrow \text{invisible} < 7.8 \times 10^{-5}$  [15]. Systematic uncertainty is estimated to be 7.9% using control samples  $B^{0,\pm} \rightarrow B^{*,\pm} l\nu$ .

$B^0 \rightarrow \text{invisible } \gamma$  decays are searched by counting events in  $E_{\text{ECL}}$  signal box in the bins of squared missing mass defined as:

Component	Yields
Signal	$18.8^{15.3}_{-14.5}$
Generic $B$	$68.1^{12.2}_{-11.7}$
Non- $B$	$-3.9^{19.5}_{-17.5}$

**Table 1:** Fitting yield ( $B^0 \rightarrow$  invisible).

	$N_{\text{bkg,box}}^{\text{data}}$	$N_{\text{box}}^{\text{data}}$
$B^0 \rightarrow$ invisible $\gamma$	$16.1 \pm 6.3$	11
$M_{\text{miss}}^2 < 5 \text{ GeV}^2 c^4$	$3.2 \pm 2.1$	2
$5 \text{ GeV}^2 c^4 < M_{\text{miss}}^2 < 10 \text{ GeV}^2 c^4$	$1.0 \pm 0.8$	2
$10 \text{ GeV}^2 c^4 < M_{\text{miss}}^2 < 15 \text{ GeV}^2 c^4$	$4.4 \pm 2.6$	3
$15 \text{ GeV}^2 c^4 < M_{\text{miss}}^2 < 20 \text{ GeV}^2 c^4$	$7.1 \pm 2.9$	4
$20 \text{ GeV}^2 c^4 < M_{\text{miss}}^2$	$6.6 \pm 2.9$	7

**Table 2:** Estimated number of background events in the signal box ( $N_{\text{bkg,box}}^{\text{data}}$ ) and the number of events in the signal box ( $N_{\text{box}}^{\text{data}}$ ) for  $B^0 \rightarrow$  invisible  $\gamma$  and  $M_{\text{miss}}^2$  bins.

$$M_{\text{miss}}^2 = P_{\text{beam}} - P_{B_{\text{tag}}} - P_{\gamma}^2 c^2, \quad (2)$$

where  $P_{\text{beam}}$ ,  $P_{B_{\text{tag}}}$  and  $P_{\gamma}$  are four-momenta of  $ee^-$  system, the  $B_{\text{tag}}$  and the signal photon. The number of background events in the  $E_{\text{ECL}}$  signal box is estimated from the data sideband by multiplying the fraction of events in signal box to the sideband, estimated in the MC. The counting results in  $E_{\text{ECL}}$  signal box and in bins of  $M_{\text{miss}}^2$  are summarized in Table. 2. The observed number of events is consistent with no signal. We set a 90% CL upper limit on the branching fraction  $\mathcal{B}B^0 \rightarrow$  invisible  $\gamma < 1.6 \times 10^{-5}$  [15] with an associated systematic uncertainty of 8.4%.

## 5. Conclusions

In summary, we have used the full data sample recorded by the Belle experiment at  $\Upsilon 5S$  and  $\Upsilon 4S$  resonances to search for the decays  $B_s^0 \rightarrow \eta' \eta$  and  $B^0 \rightarrow$  invisible  $\gamma$  and no evidence is found. We set world's first upper limits on the branching fraction of  $B_s^0 \rightarrow \eta' \eta$  and improved the existing upper limit on  $B^0 \rightarrow$  invisible  $\gamma$ .

## References

- [1] E. Kou *et al.* (Belle II Collaboration), Prog Theor Exp Phys **2019**, 123C01 (2019).
- [2] Y.-K. Hsiao, C.-F. Chang, and X.-G. He, Phys. Rev. D **93**, 114002 (2016).
- [3] A. Dedes, H. Dreiner, and P. Richardson, Phys. Rev. D **65**, 015001 (2001).
- [4] A. Badin and A. A. Petrov, Phys. Rev. D **82**, 034005 (2010).
- [5] G. Buchalla and A. J. Buras, Nucl. Phys. **B400**, 225 (1993).

- [6] B. Bhattacharya, C. M. Grant, and A. A. Petrov, *Phys. Rev. D* **99**, 093010 (2019).
- [7] C. D. Lu and D. X. Zhang, *Phys. Lett. B* **381**, 348 (1996).
- [8] A. Abashian *et al.* (Belle Collaboration), *Nucl. Instrum. Methods Phys. Res. Sect. A* **479**, 117 (2002); also see Section 2 in J. Brodzicka *et al.*, *Prog. Theor. Exp. Phys.* **2012**, 04D001 (2012).
- [9] S. Kurokawa and E. Kikutani, *Nucl. Instrum. Methods Phys. Res. Sect. A* **499**, 1 (2003), and other papers included in this Volume; T. Abe *et al.*, *Prog. Theor. Exp. Phys.* **2013**, 03A001 (2013) and references therein.
- [10] C. Oswald *et al.* (Belle Collaboration), *Phys. Rev. D* **92**, 072013 (2015).
- [11] The Fox-Wolfram moments were introduced in G. C. Fox and S. Wolfram, *Phys. Rev. Lett.* **41**, 1581 (1978). The Fisher discriminant used by Belle, based on modified Fox-Wolfram moments, is described in K. Abe *et al.* (Belle Collaboration), *Phys. Rev. Lett.* **87**, 101801 (2001) and K. Abe *et al.* (Belle Collaboration.), *Phys. Lett. B* **511**, 151 (2001).
- [12] J. Neyman, *Phil. Trans. Roy. Soc. Lond.* **A236**, 767, 333 (1937); Reprinted in *A Selection of Early Statistical Papers of J. Neyman*, (University of California Press, Berkeley, 1967).
- [13] A. Stuart and J.K. Ord, *Classical Inference and Relationship*, 5th ed., Kendall's Advanced Theory of Statistics, Vol. 2 (Oxford University Press, New York, 1991); see also earlier editions by Kendall and Stuart.  
W.T. Eadie, D. Drijard, F.E. James, M. Roos, and B. Sadoulet, *Statistical Methods in Experimental Physics*, (NorthHolland, Amsterdam, 1971).
- [14] M. Feindt, F. Keller, M. Kreps, T. Kuhr, S. Neubauer, D. Zander, and A. Zupanc, *Nucl. Instrum. Methods Phys. Res., Sect. A* **654**, 432 (2011).
- [15] Y. Ku *et al.* (Belle Collaboration), *Phys. Rev. D* **102**, 012003 (2020).